E. C. Cobb

T.-C. Cheu

J. Hoffman

Textron Lycoming,
Stratford, CT 06497

Optimal Circumferential Placement of Cylindrical Thermocouple Probes for Reduction of Excitation Forces

This paper presents a design methodology to determine the optimal circumferential placement of cylindrical probes upstream of a turbine stage for reduced excitation forces. The potential flow forcing function generated by the probes is characterized by means of a Fourier analysis. A finite difference formulation is used to evaluate the sensitivity of the forcing function to the probe positions. An optimization scheme, based on the linear programming method, uses the sensitivity analysis results to reposition the probes such that the Fourier amplitudes of critical excitation orders are reduced. The results for a sample design situation are presented.

Introduction

Technological advances in material science and internal aerodynamics are quickly exploited by the gas turbine industry to produce more efficient and lighter weight products. This results in engine operation at higher mechanical stress levels, thus demanding more accurate estimations of stress in both steady and dynamic states. This has resulted in continuous efforts to improve the state of the art in stress analysis.

The need for more sophisticated approaches, with regard to structural dynamics and vibratory stress, is particularly strong. Estimation of vibratory stress in the turbine or compressor blades of an engine during the paper design phase was once considered to be extremely difficult. Now, however, such considerations are becoming a matter of routine. In advancing such effort, methods for determining critical speeds and the deformations and stress profiles of particular modes of vibration have been developed. In short, significant progress has been made in addressing the response side of this issue. In this paper the forcing function side of vibratory stress analysis is addressed.

The vibratory response of a structural system can be mitigated by reducing the magnitude of the dynamic force that impels its motion. In general, such an approach has not been considered practical. However, for certain rather common causes, this approach can be put to use with good results. Specifically, for the case of upstream flow obstructions, produced by essential instrumentation (such as thermocouple probes), the vibratory stress induced on turbine blades resulting from wake perturbations can be estimated and systematically altered by analytic methods. Such a method is the subject of this paper. This is accomplished by application of linear programming techniques [1, 2], through which optimal values of forcing function spectral distribution and magnitude may be obtained.

It is well known that obstructions in a flow stream will create wakes behind the obstructions. Within the wakes, the pressure can drop from that of the free-stream pressure to the thermodynamic static pressure. A turbine blade passing through such a wake will be subject to a pressure variation, which can induce the unwanted vibratory response of the blade. In this paper we consider a set of cylindrical thermocouple probes placed immediately upstream of the turbine blades. These probes will create wakes, which give rise to a variable circumferential pressure, which in turn acts as forcing function on the blade.

The probe wake widths are assumed proportional to the diameter of the probes. The wake is also assumed to maintain a constant width as it travels downstream. That is, the wake does not spread out or decay. For small axial distances between the probes and the blades, as is the case in most modern turbine engines, this closely represents the true physical situation.

The general equation of motion for the blade considered as a multiple degree of freedom system is

$$[M]\ddot{\mathbf{U}} + [C]\dot{\mathbf{U}} + [K]\mathbf{U} = \mathbf{F}(t) \tag{1}$$

The excitation forces generated by the variable circumferential pressure may be characterized by means of a Fourier series analysis. Thus, the right-hand side of Eq. (1) is given by

$$\mathbf{F}(t) = \mathbf{P} \sum_{n=1}^{\infty} C_n \cos\left(n\Omega t + \phi_{n_r}\right) \tag{2}$$

With the excitation forces in this form, the steady-state solution to Eq. (1) is given by

Contributed by the International Gas Turbine Institute and presented at the 37th International Gas Turbine and Aeroengine Congress and Exposition, Cologne, Germany, June 1–4, 1992. Manuscript received by the International Gas Turbine Institute February 11, 1992. Paper No. 92-GT-423. Associate Technical Editor: L. S. Langston.

$$\mathbf{U}(t)=\sum_{n=1}^{\infty}\sum_{r=1}^{N_m}\left(\frac{\Phi_r(\Phi_r^T\cdot\mathbf{P})}{K_r}\right)[D_r]C_n\cos(n\Omega t-\phi_{n_r}) \quad (3)$$

where

$$D_r=\left[\frac{1}{\sqrt{(1-R_r^2)^2+(2\zeta_r R_r)^2}}\right]$$

$$R_r=\frac{n\Omega}{\omega_r} \quad (4)$$

as presented by Craig [3]. The complete solution to Eq. (1) will include the transient response of the system to the initial conditions. Transient response is an important part of the impulsive reaction to probe perturbation. However, transient response analysis is not treated in this paper in order that the impact of the optimization scheme on the steady-state response may be clearly demonstrated.

If the excitation forces generated by the variable circumferential pressure coincide with a natural frequency of the blade, then large resonant responses will occur. The usual solution to this problem is to redesign the turbine blades such that the blade is insensitive to the exciting forces. Since aerodynamic design constraints on the blades do not generally allow radical changes in the blade geometry, an effective design change is often hard to come by. This is particularly true of power turbine blades where there are no internal cavities that could be modified to provide some relief [4].

When modification of the blade structure is not possible, the only feasible solution is to reduce or change the forcing function acting on the blades. To accomplish this effectively, a systematic technique of parameter iteration must be used, whereby an optimization of effects is achieved. By using such optimization techniques, design parameters that are not aerodynamically related to performance can be adjusted to alter the shape of circumferential pressure variations. The adjustments are made such that a reduction of the amplitudes of those Fourier components of the forcing function (produced by that shape) can be effected. Most important among these are the ones that can generate blade resonance. In effect, the energy associated with the resonant components is shifted to less critical modes.

In this study, the design parameters selected are the circumferential locations of the thermocouple probes. The locations of each probe is assumed to be unrestricted, except that the probes may not physically overlap or have excessive movement such that the proper measurements of circumferential temperature distributions for engine control are lost. Additional proscriptions may be imposed on the specific probe locations by some other design criteria, such as avoiding fuel lines or oil service lines.

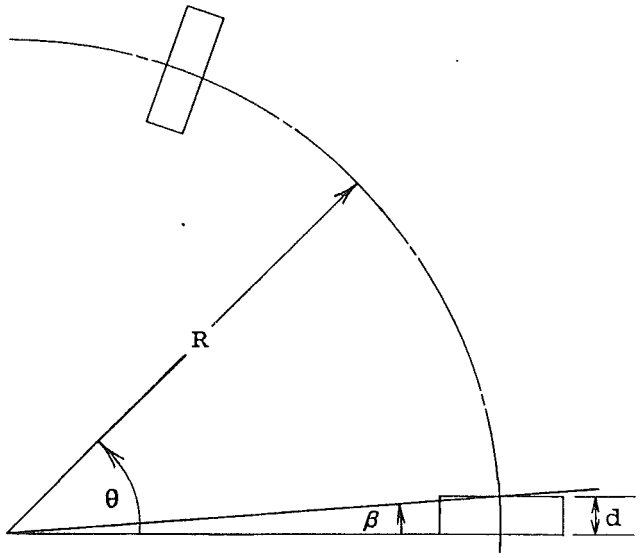

Fig. 1 Geometry parameters for circumferential placement of the thermocouple probes

The circumferential pressure pattern in a plane downstream of the probes is defined as a specific pressure, P_p, at a given angle of circumference. The circumferential pressure pattern between the probes is assumed to be constant and is equal to the free-stream pressure, P_s. The pressure in the wake behind the probes is assumed to drop to a minimum pressure equal to the thermodynamic static pressure, P_0.

The width of the pressure wake downstream of a probe is assumed to be equal to the diameter of the probe. Figure 1 shows the geometry definitions used in defining the wake width at the midspan of the probe. The angle that subtends the circumferential arc length at the probe midspan radius is defined as β and is given by

$$\beta=2\tan^{-1}\frac{d}{2R} \quad (5)$$

This angle will increase as the radial position from the engine

Nomenclature

A_n = coefficients of the Fourier cosine terms
B_n = coefficients of the Fourier sine terms
C_n = vector amplitude of the Fourier coefficients
$[C]$ = structural damping matrix
D_r = modal amplification factor
d = probe diameter
f = objective function
$\mathbf{F}(t)$ = vector of time-dependent forcing function
g = constraint functions
i, j = indices
$[K]$ = structural stiffness matrix
K_r = modal stiffness
$[M]$ = structural mass matrix
M = number of spatial divisions within a wake
N = number of movable probes
N_m = number of modes to be used in the modal analysis
N_f = number of frequencies to be constrained
n = integer value of the excitation order
$\mathbf{P}$ = vector defining the spatial dependence of the loading
P_0 = minimum pressure within the wake behind a probe
P_p = pressure magnitude within the wake behind a probe
P_s = free-stream pressure between probes
q = number of spatial increments
r = variable index of the natural frequency mode number
R_r = frequency ratio = Ω/ω_r
$\mathbf{U}(t)$ = displacement vector of physical coordinates
α = design variable
β = angle subtending the arc length of the probe diameter
ϵ = integration error
θ = circumferential angle
ζ_r = modal damping factor for the rth mode
Φ_r = normal mode shape for the rth mode
ϕ_{nr} = phase angle of the nth excitation order in the rth normal mode
Ω = rotational speed of the rotor
ω_r = natural frequency of the rth mode

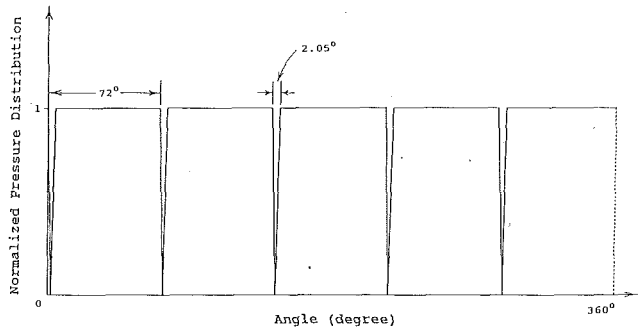

Fig. 2 Pressure pattern for five equally spaced circumferential thermocouple probes with 0.25 in. probe diameter and 7.0 in. radius at midspan of the probes

centerline is decreased. Thus, the optimization analysis is also a function of the particular radius from the engine centerline used. The methodology presented here does not currently account for the change in the Fourier coefficients as a function of the radius. However, this was judged to be a tolerable modeling expedient. The analysis for the example given in this paper was performed at the midspan radius of the probe, which gives a good approximation of the total forcing function.

The pressure in the wake downstream of a probe varies with the circumferential angle. The angle β is normalized to range from zero to π so that the pressure is represented by a sine squared function using the normalized angle, that is

$$P_p = (P_s - P_0)\left(1 - \sin^2\left(\frac{i\pi}{M}\right)\right) \quad i = 0 \ldots M \tag{6}$$

where M is the number of divisions of β. Experimental testing has shown that this mathematical definition of the pressure is quite accurate [5].

As an example, the circumferential pressure distribution shown in Fig. 2 is given for the case where the pressure difference between the free-stream pressure and the static pressure is normalized to one. There are five identical probes of 0.635 cm (0.25 in.) diameter, spaced 72 deg apart, and at a radius of 17.78 cm (7.0 in.).

Fourier Analysis

For a given number of probes at specified circumferential locations, the resulting pressure versus circumferential angle for a complete traverse of the turbine stage can be developed and represented by a Fourier series [6]. In the general case, this pressure pattern will have a spatial period equal to the probe mid span circumference, or in angular measure, 2π. Thus:

$$P_p(\theta) = A_o + \sum_{n=1}^{\infty} \{A_n \cos(n\theta) + B_n \sin(n\theta)\} \tag{7}$$

The Fourier coefficients of the pressure pattern may now be evaluated using the well-known Euler formulas:

$$A_o = \frac{1}{2\pi}\int_{-\pi}^{\pi} P_p(\theta)d\theta$$

$$A_n = \frac{1}{\pi}\int_{-\pi}^{\pi} P_p(\theta)\cos(n\theta)d\theta$$

$$B_n = \frac{1}{\pi}\int_{-\pi}^{\pi} P_p(\theta)\sin(n\theta)d\theta \tag{8}$$

The pressure pattern may also be described in the vector amplitude form:

$$P_p(\theta) = \sum_{n=1}^{\infty} C_r \cos(n\theta + \phi_n) \tag{9}$$

where

$$C_n = \sqrt{A_n^2 + B_n^2}$$

$$\phi_n = \tan^{-1}\frac{B_n}{A_n} \tag{10}$$

Using simple numerical integration methods, the Fourier series coefficients described in Eq. (8) can be easily obtained for a specific pressure distribution. A Simpson's rule numerical integration scheme was used in this study to evaluate the Fourier coefficients.

In the frequency domain, the forcing function can be specified conveniently by these Fourier coefficients. Derivatives of the Fourier coefficients with respect to the locations of the probes provide the trend of variation of the amplitudes of various excitation modes due to the change of probe locations. These derivatives are required by the linear programming technique to find the optimal placement of the probes for reduced excitation.

Analysis Procedure

The problem of the optimal placement of thermocouples can be stated as to minimize an objective function, f, which can be selected as the amplitude of the most critical mode, subject to the design constraints on selected modal amplitudes, of:

$$g_j^L \le g_j \le g_j^U \qquad j = 1, \ldots, N_f \tag{11}$$

and the side constraints of the design variables

$$\alpha_i^L \le \alpha_i \le \alpha_i^U \qquad i = 1, \ldots, N \tag{12}$$

where N is the total number of movable probes and the design variables are selected as angular locations of the probes.

Using the first-order Taylor series expansion centered at the current locations, f and g of the new placement can be approximated as

$$f = f_0 + \sum_{i=1}^{N} \frac{\partial f}{\partial \alpha_i}(\alpha_i - \alpha_{io}) \tag{13}$$

$$g_i = g_{jo} + \sum_{i=1}^{N} \frac{\partial g_i}{\partial \alpha_i}(\alpha_i - \alpha_{io}) \quad j = 1, \ldots, N_f \tag{14}$$

to form a linear programming problem over a limited range of design variables. Calculations of the derivatives of the objective function and the constraint functions are called sensitivity analyses because these derivatives provide the trend of variations of those functions due to the change in the design variables. In this paper these derivatives are calculated using a central finite difference formulation presented in the following.

When using central finite difference to perform sensitivity analysis, the derivatives are calculated for each design variable one at a time. All of the probes except the one for which the derivative is being calculated are considered fixed. For the design variable associated with the movable probe, a small perturbation in the circumferential location is added to and to and subtracted from the current probe location. The Fourier coefficients are evaluated for the modified circumferential pressure patterns resulting from these positive and negative perturbations. The derivatives of the coefficients with respect to the probe location are approximated by the change in the Fourier coefficient amplitudes divided by twice the perturbation. For the nth vector amplitude, the derivative with respect to the ith design variable is:

$$\frac{\partial C_n}{\partial \alpha_i} \approx \frac{C_n(+\Delta\alpha_i) - C_n(-\Delta\alpha_i)}{2\Delta\alpha_i} \quad \begin{matrix} n = 0, 1, \ldots, \infty \\ i = 1, 2, \ldots, N \end{matrix} \tag{15}$$

The derivatives of A_n and B_n may also be calculated in the same manner.

Sample Problem

The methodology developed above was implemented by a FORTRAN program for automatic computation. As a sample case, the situation of a thermocouple harness containing five probes upstream of a turbine stage in a small gas turbine engine was analyzed. The probes were uniformly spaced at 0, 72, 144, 216, and 288 deg. All five probes were given the same diameter, 0.635 cm (0.25 in.). The pressure difference between the free-stream pressure and the static pressure was normalized to one. The analysis is carried out at the midspan radius of the probes which was defined as 17.78 cm (7.0 in.). Figure 2 shows the resulting idealized circumferential pressure distribution for this example. The turbine blades were considered to be sensitive to the fifth-order excitation at the operating rotational speed. The design goal was to reduce the magnitude of the fifth-order excitation generated by the thermocouple probe wakes.

As a practical matter, it is not feasible to compute every term in the displacement solution summation of Eq. (3). In addition, for practical engineering problems, not every Fourier coefficient is required to be constrained. Thus, we impose limits only on the excitation orders immediately above and below the critical excitation order. This is an acceptable approximation as a result of the inverse square relationship of the response to the frequency ratio given in Eq. (3). Because of this relationship, energy transferred to excitation orders other than those in immediate proximity of the critical order will have little effect on the response. Therefore, because the fifth-order excitation was specified as the critical excitation order in the example, only the fourth and sixth excitation order coefficients are required to be constrained. However, in order to demonstrate the capacity of the software developed, the first through fourth and the sixth through ninth excitation order coefficients are constrained to have an upper limit of 0.01 on their amplitudes.

Additional constraints due to the locations of other mechanical components were: Because of an oil supply line, the number one probe (located at 0.0 deg) was not permitted to move in the clockwise direction, and, because of a structural support, the number five probe (located at 288 deg) was also not allowed to move in the clockwise direction.

To perform the numerical integration to calculate the Fourier coefficients, an initial spatial increment of ten points per degree of circumference was selected. Using the selected spatial increment, the circumferential pressure pattern was discretized. The discretization process yields a total of 3600 spatial points in one period and allows 1800 Fourier coefficients to be computed. The reconstruction of the actual pressure distribution requires an infinite series summation of the Fourier coefficients and their associated functionals. However, as indicated before, each of the individual Fourier coefficients is calculated with a high degree of accuracy because of the number of points used to define the function in the spatial domain. Therefore, only those coefficients and their derivatives pertinent to the objective and constraint functions require calculation.

The present example used three design variables. The three design variables selected, α_1, α_2, and α_3, were the locations of probe numbers 1, 3, and 5, respectively. The objective was to reduce the amplitude of the fifth-order coefficient while constraining the amplitudes of the first through fourth and the sixth through ninth-order coefficients to be less than or equal to 0.01 psi. At the same time, geometry constraints are placed on the maximum motion (in degrees) that the design variables may move.

Therefore, the objective function is stated simply as:

$$f = C_5 \tag{16}$$

while the constraint functions are defined by:

$$C_i \le 0.01 \qquad \begin{matrix} i = 1, 2, 3, 4, \\ 6, 7, 8, 9, \end{matrix} \tag{17}$$

and the side constraints on the probe locations are given by:

$$\begin{aligned} -1 \le \alpha_1 \le 0 \\ -1 \le \alpha_2 \le 1 \\ -1 \le \alpha_3 \le 0 \end{aligned} \tag{18}$$

These side constraints prevent the first and fifth probes from moving in the clockwise direction (positive changes of α_1 and α_3) but allow the third probe to move in either direction. These side constraints also serve as the maximum move limits of design variables used for each iteration in the linear programming. By experience, these move limits allow the functions to be linearized to give a good approximation of the nonlinear characteristics of the problem while retaining a reasonable computation cost.

The computation results for this example are presented in Tables 1–7. The computation proceeded through three global iterations, each with a different integration increment size. There are a number of local iterations within each global iteration. The local iterations of each global iteration are considered converged when all the movable probes cannot move with an angle larger than the integration increment size of the associated global iteration. A final global iteration is performed with a very small integration increment size to verify that the analysis has converged.

The integration increment size is fixed within each global iteration. However, the integration increment size is reduced by an order of magnitude when computation proceeds from

Table 1 Change of probe locations (deg) for the first global iteration

Iteration Number	Probe Number 1	2	3	4	5
1	0.0000000	0.0000000	1.0000000	0.0000000	0.0000000
2	-1.0000000	0.0000000	1.0000000	0.0000000	-1.0000000
3	-1.0000000	0.0000000	1.0000000	0.0000000	-1.0000000
4	-1.0000000	0.0000000	1.0000000	0.0000000	-1.0000000
5	0.0000000	0.0000000	1.0000000	0.0000000	-1.0000000
6	0.0000000	0.0000000	1.0000000	0.0000000	-0.2000000
7	0.0000000	0.0000000	0.1000000	0.0000000	0.0000000
8	0.0000000	0.0000000	0.0000000	0.0000000	0.0000000

Table 2 Change of probe locations (deg) for the second global iteration

Iteration Number	Probe Number 1	2	3	4	5
1	0.0000000	0.0000000	0.9500000	0.0000000	0.0000000
2	0.0000000	0.0000000	0.0400000	0.0000000	0.0000000
3	0.0000000	0.0000000	0.0000000	0.0000000	0.0000000

Table 3 Change of probe locations (deg) for the third global iteration

Iteration Number	Probe Number 1	2	3	4	5
1	0.0000000	0.0000000	1.0000000	0.0000000	0.0000000
2	0.0000000	0.0000000	0.2470000	0.0000000	0.0000000
3	0.0000000	0.0000000	0.0290000	0.0000000	0.0000000
4	0.0000000	0.0000000	0.0230000	0.0000000	0.0000000
5	0.0000000	0.0000000	0.0080000	0.0000000	0.0000000
6	0.0000000	0.0000000	0.0000000	0.0000000	0.0000000

Table 4 Probe locations (deg) for the global iterations

Iteration Number	Probe Number 1	2	3	4	5
0	0.000000	72.000000	144.000000	216.000000	288.000000
1	-3.000000	72.000000	150.100000	216.000000	283.800000
2	-3.000000	72.000000	151.090000	216.000000	283.800000
3	-3.000000	72.000000	152.397000	216.000000	283.800000

Table 5 Harmonic amplitudes for the first global iteration

Iteration Number	Harmonic Amplitude (10^{-3}) C_0	C_1	C_2	C_3	C_4	C_5	C_6	C_7	C_8	C_9
1	985.7877	0.1513	0.1540	0.1564	0.1578	28.3848	0.1648	0.1641	0.1678	0.1683
2	985.7877	0.2398	0.2026	0.3030	0.5238	28.3647	0.7463	0.6293	0.7930	1.0074
3	987.0519	2.7436	2.2826	2.9369	1.8656	25.7641	3.9559	1.8865	3.6298	1.9934
4	988.6292	6.0608	5.3680	6.2035	4.3708	22.4301	7.9151	4.9831	7.0553	3.4160
5	988.6302	6.2201	5.3172	6.3213	3.9343	22.1718	8.8021	5.3040	7.2367	3.6619
6	988.6302	6.3781	5.2760	6.4329	3.6155	21.8331	9.6281	5.8870	7.2993	4.5743
7	988.6302	6.4572	5.1481	6.6901	3.4842	21.5772	9.9717	6.2187	7.7950	5.0551
8	988.6307	6.4622	5.1341	6.7193	3.4732	21.5527	9.9928	6.2495	7.8548	5.0863

Table 6 Harmonic amplitudes for the second global iteration

Iteration Number	Harmonic Amplitude (10^{-3}) C_0	C_1	C_2	C_3	C_4	C_5	C_6	C_7	C_8	C_9
1	988.6312	6.4019	5.2564	6.7752	3.0852	21.5775	9.8151	6.4922	7.8632	4.9003
2	988.6312	6.4509	5.1348	7.0473	2.9659	21.3475	9.9924	6.8554	8.4022	5.2290
3	988.6312	6.4527	5.1303	7.0594	2.9613	21.3373	9.9992	6.8729	8.4241	5.2429

Table 7 Harmonic amplitudes for the third global iteration

Iteration Number	Harmonic Amplitude (10^{-3}) C_0	C_1	C_2	C_3	C_4	C_5	C_6	C_7	C_8	C_9
1	988.6312	9.2801	8.6817	9.0439	2.2201	21.5067	9.8259	7.1561	8.3794	4.8395
2	988.6312	9.2473	8.6910	9.2649	1.8381	21.2365	9.9703	7.6561	8.8714	5.2421
3	988.6312	9.2408	8.6975	9.3132	1.7462	21.1676	10.0020	7.7924	8.9865	5.3408
4	988.6312	9.2433	8.6971	9.3072	1.7570	21.1757	9.9983	7.7761	8.9730	5.3293
5	988.6312	9.2410	8.6976	9.3122	1.7484	21.1692	10.0012	7.7890	8.9838	5.3384
6	988.6312	9.2415	8.6972	9.3105	1.7513	21.1716	10.0002	7.7845	8.9800	5.3353

one global iteration to the next. The analysis within the first global iteration uses an integration increment size of 0.1 deg. Once the local iterations converge, the step size is reduced to 0.01 deg. The second global iteration then continues beginning from the probe positions determined in the last global iteration. The smaller integration increment size increases the accuracy of the Fourier coefficient calculation and the sensitivity analysis. Therefore, the algorithm may move the probes a larger amount in the local iteration immediately following the integration increment size change. However, the trend of convergence is always in toward the order of the step size. The analysis proceeds within the seconds global iteration until the local iterations converge. The integration increment size is reduced further to 0.001 deg and the analysis continues until the local iteration converges. Tables 2 and 3 clearly show this behavior occurring in the first local iteration after the integration increment size change for both the second and third global iterations.

In our example, the overall program was considered converged when the change in location of any one of the movable probes was less than 0.001 deg. This limit was set from the practical consideration that angles smaller than this cannot easily be measured in a manufacturing situation. This convergence criterion was reached after the third global iteration. A final global iteration was run with a very small integration step size of 0.0005 deg. Since the changes of all of the probe locations were zero at the first local iteration of the fourth global iteration, it was verified that the algorithm had converged.

Table 4 shows an iteration history of the probe locations. For each iteration, the change in the angular location of each probe is given. Because their position specifications are fixed, there are no changes in the locations of the number 2 and 4 probes.

Tables 5–7 show the iteration history of the harmonic amplitudes. Figure 3 is a histogram showing the change in the

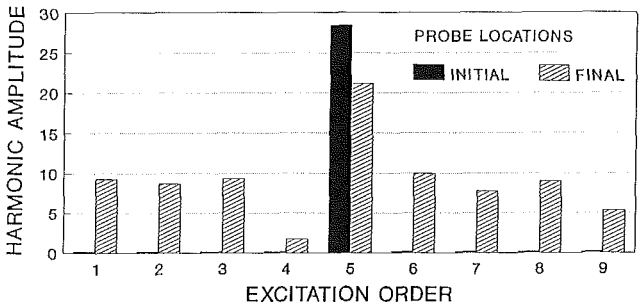

Fig. 3 Initial and final vector amplitudes for the example

vector amplitudes of the first nine excitation orders between the condition at the beginning of the analysis and the condition at the conclusion of the analysis. After three global iterations, amplitude of the fifth-order excitation has been reduced by 26 percent. The amplitudes of all other excitation orders have been increased and are approaching the constraint upper limit. The amplitudes of the first, second, third, sixth, and eighth-order excitations have closely approached the constraint upper limit of 0.01 psi. Because the amplitudes of these coefficients are approaching the upper limit, an alternate convergence criterion could be specified by defining a tolerance bound on these constraint amplitudes.

Three simple examples of the application of the methodology are represented in the Goodman diagram shown in Fig. 4. For a linear system, a 26 percent reduction in the excitation force will result in a 26 percent reduction in the alternating stress.

Consider the following three hypothetical cases. The first case is an engine component with a mean stress of 25 ksi, and an alternating stress of 11 ksi, point A in Fig. 4. Assuming that the contributions to the alternating stress from excitation orders other than the fifth order are negligible, a reduction of 26 percent in the alternating stress brings the alternating stress

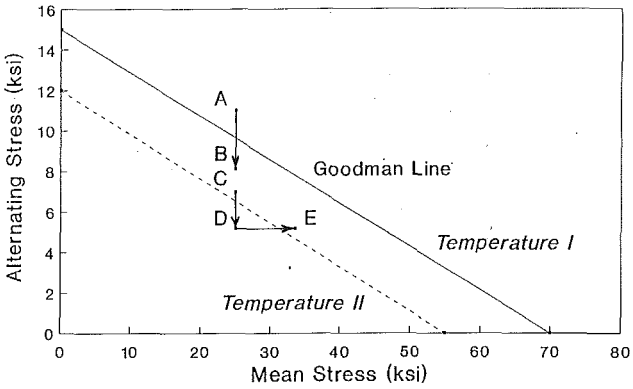

Fig. 4 Goodman diagram for the sample problem

to 8.14 ksi, or point B in Fig. 4. Using the Goodman line at temperature I, Fig. 4 clearly shows that such a reduction in alternating stress brings the component from the finite life region to the infinite life region.

The second case again uses the Goodman line at temperature I. This case is that of an engine component with a mean stress of 25 ksi and an alternating stress of 7 ksi, point *C* in Fig. 4. This stress condition provides a vibratory margin of 2.64 ksi. A reduction of the alternating stress by 26 percent brings the alternating stress to 5.18 ksi, point *D*. In this case the mean stress may safely be increased to 33.5 ksi while retaining an infinite life of the component and maintaining a vibratory margin of 2.64 ksi. This increase in allowable mean stress means that the component could be operated safely at a speed 16 percent higher, thus improving performance without sacrificing component life or vibratory margin.

The third case is that where the engine component also has an alternating stress of 7 ksi and a mean stress of 25 ksi. With a 26 percent reduction of the alternating stress, from 7 ksi to 5.18 ksi, and a constant mean stress, the temperature of the component could be increased. With an increase in temperature, the Goodman line would move from that given by the temperature *I* line to that at temperature *II*, the dashed line shown in Fig. 4. An increase in the overall temperature of the engine will result in improved performance. By reducing the forcing function acting on the blades, the alternating stress in the blades will be reduced. A temperature increase to improve engine performance can then be made without sacrificing component life.

All three of these examples demonstrate a marked improvement in the quality of the components resulting from reduction of the forcing function driving the vibration of the components. The application of this methodology allows any one or a combination of all three improvements to be made to an engine component.

Conclusion

A methodology has been presented that provides a simple and powerful automated tool for use in reducing the amplitude of the excitation generated by thermocouple probes upstream of a turbine rotor. Using this methodology, the aerodynamic parameters upstream of the probes are not altered. Therefore, the aerodynamic performance of the engine is impacted minimally. The methodology presented is capable of handling a large spectrum of complex design situations. The methodology associated with this type of problem. This is accomplished by providing a computational approach for determining the locations of thermocouple probes to reduce the downstream wake excitation amplitudes. The algorithm itself is highly efficient. The example given in this paper was executed on an IBM 3090 mainframe computer using 14.4, 53.4, 460.2 CPU seconds for the first, second, and third global iterations respectively. The verification run required 145.2 CPU seconds to confirm the convergence of the solution.

The methodology can be extended in the following manner. First, the methodology can be adapted to consider other objects in the flow path. The methodology has general applicability if the pressure wake downstream of the obstruction can be described in a piecewise analytic manner. Thus excitations generated by stator vanes or inlets or inlet struts may also be considered by the methods presented here. Secondly, a pseudo-three-dimensional analysis may be conducted by including the effects of various radii on the Fourier coefficients. Finally, a transient response analysis can be included, if desired, by including the system initial conditions in the solution of Eq. (1).

In summary, this paper presents an effective and efficient methodology to improve the quality and reliability of gas turbine engine components. The software developed to implement this methodology is highly accurate and cost effective. Therefore, component quality assurance can be achieved with reduced design effort.

References

1 Fox, R. L., *Optimization Methods for Engineering Design*, Addison-Wesley, Reading, MA, 1973.

2 Zienkiewicz, O. C., and Campbell, J. S., *Shape Optimization and Sequential Linear Programming, Optimum Structural Design Theory and Applications*, R. H. Gallagher and O. C. Zienkiewicz, eds., Wiley, New York, 1973.

3 Craig, R. R., *Structural Dynamics*, Wiley, New York, 1981.

4 Cheu, T. C., "Sensitivity Analysis and Shape Optimization of Axisymmetric Structures," *International Journal for Numerical Methods in Engineering*, Vol. 28, 1989, pp. 95–108.

5 Kerrebrock, J. L., and Mikolajczak, A. A., "Intra-stator Transport of Rotor Wakes and Its Effect on Compressor Performance," ASME JOURNAL OF ENGINEERING FOR POWER, Vol. 92, 1970, pp. 359–368.

6 Brigham, E. O., *The Fast Fourier Transform*, Prentice-Hall, Inc., Englewood Cliffs, NJ, 1974.

7 Ralston, A., and Rabinowitz, P., *A First Course in Numerical Analysis*, McGraw-Hill, New York, 1978.